International Journal of Nanoelectronics and Materials
Volume 11, No. 3, July 2018 [333-346]

Contemplating Nanometer Scale Transport Characteristics through Aromatic Molecules Based Molecular Devices

Rajan Vohra[1*] and Ravinder Singh Sawhney[2]

[1,2] Department of Electronic Technology, Guru Nanak Dev University, Amritsar (Punjab).

Received 26 October 2017; Revised 4 January 2018; Accepted 23 April 2018

ABSTRACT

In this research article, we contemplate the quantum transport properties through a single molecular junction comprising of Azulene ($C_{10}H_8$) sandwiched between two semi-infinite gold (Au) electrodes and compare the transport properties with its higher derivative Anthracene ($C_{14}H_{10}$) based device having similar geometrically optimized data. By modeling this device, we evaluate vital transport parameters like current, conductance, transmission spectra, HOMO-LUMO gap and rectification ratio using a combination of non-equilibrium green's function and extended Huckle formalism. We observe that Au-$C_{10}H_8$-Au device exhibit higher current in spite of having lower conductance as compared to Au-$C_{14}H_{10}$-Au device within a variegated bias range. However, Azulene based device has the advantage of getting fabricated as a molecular wire because the charge transfer through this molecule is comparatively stabilized. This property can allow us to produce a molecular diode, which in turn can give us further insight to design molecular devices which can replicate the conventional semi-conductor devices. On the other hand, Anthracene based molecular devices can be utilized in electronic applications such as organic solar cells, OLEDS (Organic Light Emitting Diodes) etc.

Keyword: Azulene, Anthracene, HOMO-LUMO Gap, Non-Equlibrium Green's Function, Extended Huckle Theory.

1. INTRODUCTION

In 1974, Aviram and Ratner [1] suggested an organic molecular system in which they observed the current rectification by composing a donor and an acceptor group joined by a carbon bridge having single bonds. Ratner later revealed [2] that the realization of such a proposal was "somewhere between science fiction and state-of-the-art". It was in mid-1990s that the first noteworthy attempt of charge transport through single molecules were reported [3,4]. At that time formation of electrode–molecule–electrode junction was not optimally feasible. Moreover, managing the unavoidable variability was also not easy to predict the properties of single molecules. In 2003, Nongjian Tao and Bingqian Xu developed a method to address these concerns. They made use of STM as an electrically active 'fishing rod' that selects up molecules from the surface of electrode [5]. The tip of STM interacts with the molecules on the surface and then slowly moves away. The molecules having end-group anchors to form the covalent bonds to both the electrode and the STM tip bridge the two. In this way, an electrode–molecule–electrode junction is formed. Molecular electronics is being anticipated as an alternative to silicon based conventional electronics in post-CMOS era. Molecules encompass distinctive functions with many applications that complement the silicon based microelectronics.

*Corresponding Author: *rajanvohraece.rsh@gndu.ac.in*

Due to this, a range of molecules possessing unique properties have been accredited for numerous molecular applications. Besides electronic properties, these molecules possess plethora of optical, magnetic, thermoelectric, electromechanical properties to construct newer devices that may never be possible using conventional approaches as shown in figure 1 [6]. In this research article, we meticulously compare the electronic and electrical characteristics of Azulene with its higher end polymer Anthracene using two-electrode molecular junction approach. In 2016, Rupan Preet Kaur et. al. [7] studied the electrical conduction through single-molecular junctions involving of Anthracene.

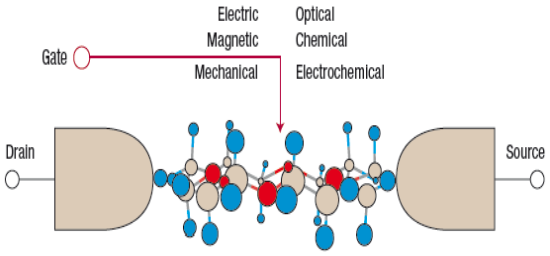

Figure 1. Illustration of a single molecule attached to two electrodes as a basic component in molecular electronics [6].

Electron transport through the molecule may be controlled electrically, magnetically, optically, mechanically, chemically and electrochemically, leading to various potential device applications. To reach the ultimate goal in device applications, experimental techniques to fabricate such an electrode–molecule–electrode junction and theoretical methods to describe the electron transport properties must be developed in conjunction to supplement each other. Both are challenging tasks and rapid advances have been made in recent years. Moreover, in 2014, Ravinder Singh Sawhney and Rupan Preet Kaur studied a geometrically enhanced method to explore the dependence of bond length, bond angle and rotation angle alternations on the conduction of an aromatic molecule anthracene considered for modelling and simulation [8]. In 2008, S. Dutta et. al., compared the electron transport phenomenon through Azulene with its isomer Naphthalene [9].

2. COMPUTATIONAL DETAILS

In this article, we contemplate the transport properties of Azulene ($C_{10}H_8$) and then differentiate with the results exhibited by Anthracene ($C_{14}H_{10}$). Azulene is an aromatic organic compound and is an isomer of naphthalene. Anthracene is a solid polycyclic aromatic hydrocarbon consisting of three fused benzene rings. We have used the Landuaer approach [10], in which one can ideally divide the molecular junction device into multiple regions (i) a central region (C) (ii) a left (L) and right (R) lead connected to the molecule; (iii) two electron reservoirs connected to the leads, in equilibrium at some electrochemical potential $\mu_{L,R}$ and is shown in figure 2.

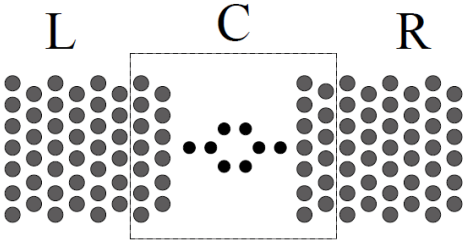

Figure 2. Typical arrangement of a two probe junction.

The left and right electrodes (L,R) are supposed to be semi-infinite electron reservoirs in equilibrium at a fixed electrochemical potential. The contact region (C, within the dashed box) includes the molecule and a small portion of the electrodes, while the metal at the edges of the contact region has bulk-like properties. The leads (often called electrodes) are assumed to be ballistic conductors, i.e. conductors with no scattering and thus having transmission probability equal to one.

The length of the electrodes is chosen to be 7 Å while electron temperature is set to 300 K. This particular length of the electrode has been selected so that there are either no or negligible interactions with the second-nearest neighbour cell in the transport direction[10]. Though several approaches to model this device have been suggested but our method has been deliberately based on mechanically control break junction technique [11-12]. It is formed by mechanically elongating the gold wire up to its breaking point. Next fractured surfaces of gold wire are cleaned. Finally these cleaned and smoothened gold electrodes are exposed to the Azulene molecule. Thus an organic molecular bridge is formed. The same process is repeated for the Anthracene. The electrodes are erected using miller indices h:k:l as 1:1:1. To study the effect of electric field on both these devices based on these molecules, we enhance the structure of Azulene and Anthracene with two thiol groups at trans-positions as shown in figure 3 [13-14].

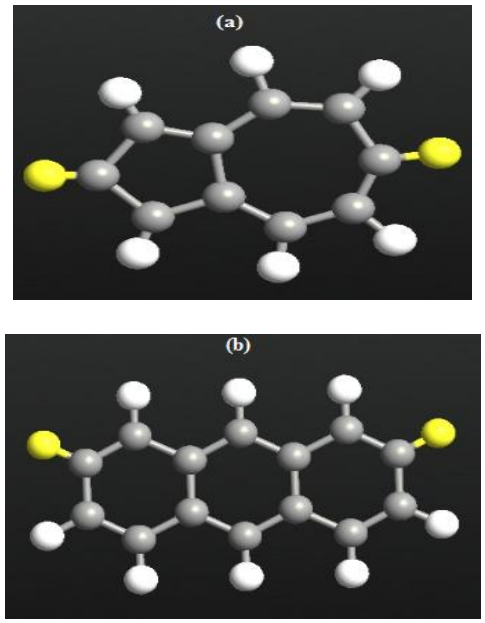

Figure 3. Structure of (a) Azulene and (b) Anthracene with two thiol groups linked at trans-positions.

The two-probe system model shown in figure 4 consists of Azulene molecule and Anthracene molecule with two thiol groups at trans-positions connected with gold electrodes. Gold as an electrode has been suggested by peer research groups earlier as well because of its unique properties of being chemically inert in air. [15]

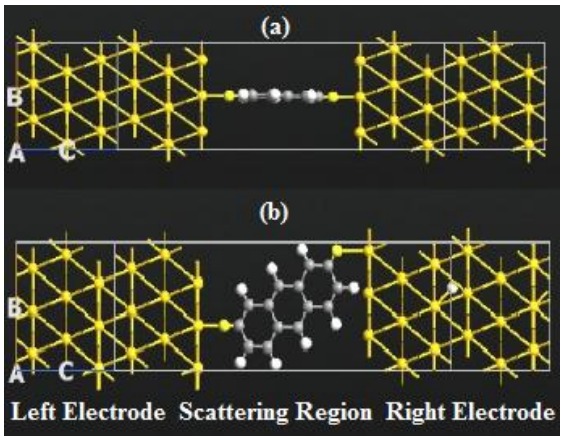

Figure 4. Molecular electrode junction with (a) Azulene molecule (b) Anthracene molecule in the central region.

The quantum transport properties of two-probe system are calculated using the semi-empirical approach based on Extended Huckel Theory (EHT) in conjunction with non-equilibrium green's function (NEGF) [16-20] duo using atomistic scale modeling software ATK version 13.8.2 [21-22]. The most distinctive property of ATK is its ability to calculate the electrical transport properties of two-probe systems and has realistically reproduced experimental data [22]. The electrostatic potentials are determined on a real-space grid with mesh cut-off energy of 75 Hartree and further quantum calculations are performed using Monkhorst-Packk-point sampling of 1 × 1 × 100 for Brillouin zone. These parameters led to calculations of two secondary parameters viz. current and conductance.

The Landuaer-Büttiker relation to calculate the current is given as

$$I = \frac{2e^2}{h}\int_{-\infty}^{+\infty} T(E)[\, n_f(E-\mu_L) - n_f(E-\mu_R) \qquad (1)$$

Where 'e' is the electron charge, 'h' is Planck's constant and is equal to 6.626 X 10^{-34} J-S, T(E) is the transmission probability (T=1 for ballistic), μ_R and μ_L are the right and left electrode chemical potential respectively.

In the Landauer approach, linear-response conductance is given by

$$G = G_0 T(E_F) \qquad (2)$$

here $G_0 = 2e^2/h$ is the fundamental quantum conductance unit that measures the conductance of quantum point contact.

3. RESULTS AND DISCUSSIONS

In this paper, the electron transport properties for Azulene and Anthracene molecular junctions are partitioned into two parts. In first part, we scrutinize the quantum transport properties for the two configurations under zero bias, to study the impact of the coupling of the Azulene and Anthracene molecules with the gold electrodes. In second part, the similar process is repeated but with variegated voltage range from -2 V to +2 V with a step size of 0.2V.

At zero bias voltage, transmission spectrum is calculated. The transmission spectrum at zero bias is the sequence of peaks having different width and height depicting the relative strength of coupling between molecule and gold electrode. Figure 5 illustrates the transmission spectra

under equilibrium condition for Au-Azulene-Au and Au-Anthracene-Au within -2 to + 2 energy range.

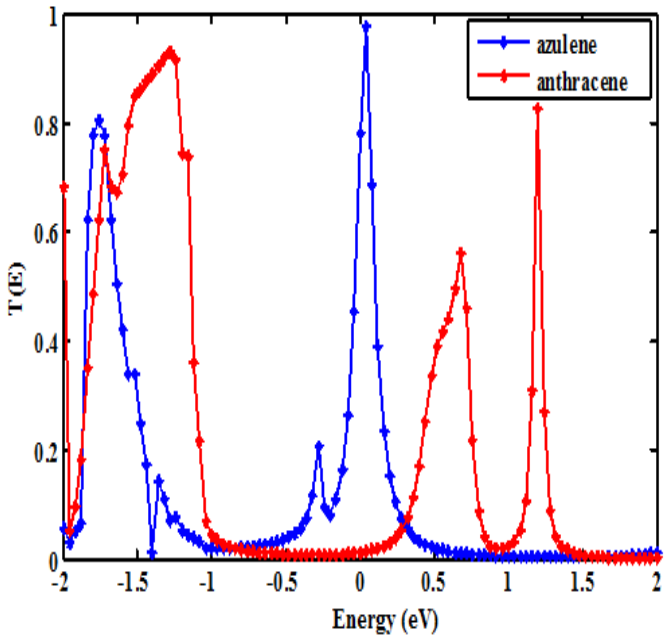

Figure 5. Transmission Spectrum at zero bias for for Au-$C_{10}H_8$-Au and Au-$C_{14}H_{10}$-Au devices.

From the comparison of transmission spectra for the two devices, it is evident that Au- $C_{10}H_8$-Au is exhibiting the sharp and highest magnitude peak in transmission window. This shows the peak is equally divided in HOMO and LUMO regions with respect to fermi level, whereas, Au-$C_{14}H_{10}$-Au shows no peak at the equilibrium state. The transmission resonance is found to be least in this case. This indicates a relatively weaker coupling of molecule to the electrodes and hence predicts lowest HLG for the applied bias range. Transmission spectra T(E) under bias voltage of -2 V to +2 V (step size 0.2) are calculated with respect to energy levels of -2 eV to + 2 eV and plotted in figure 6.

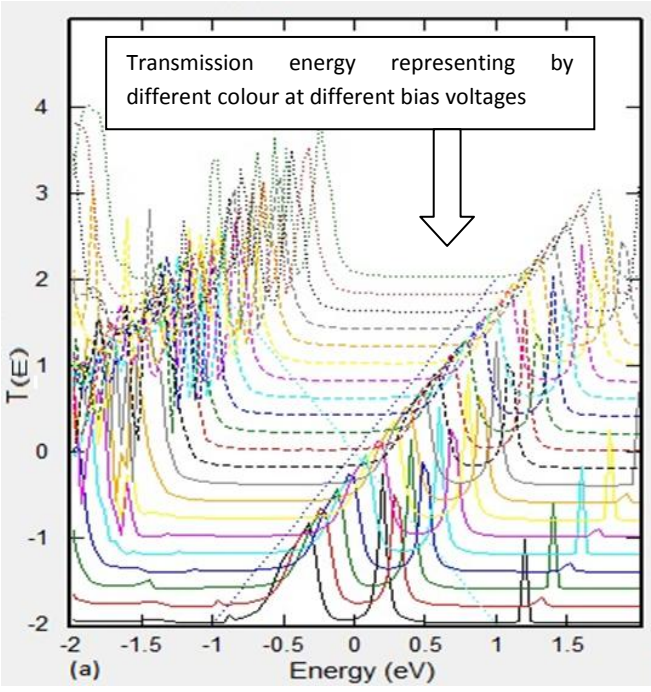

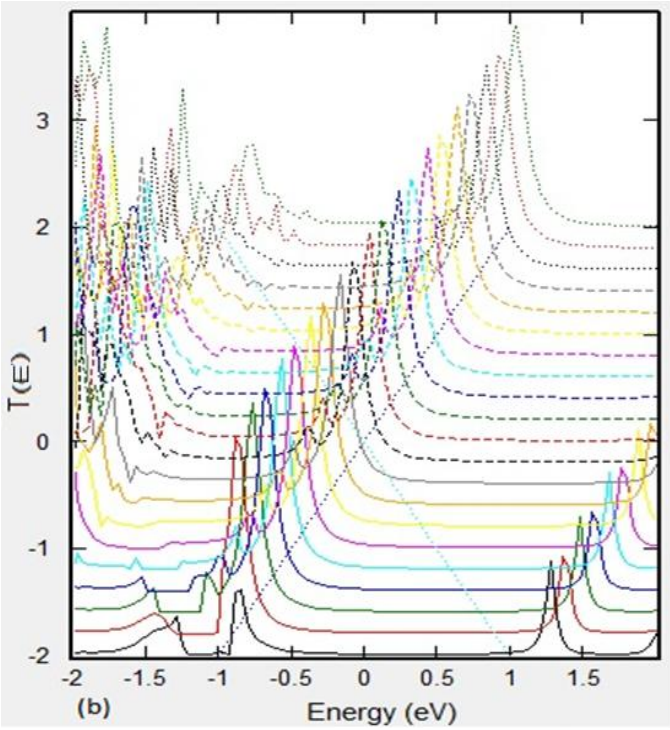

Figure 6. Transmission spectrum of the two molecular device junctions (a) Azulene (b) Anthracene.

Figure 6 exhibits the Au-Azulene-Au device, and it is evident that the conduction is through LUMO for this applied bias voltage range. This further suggests the strong binding of Azulene molecule with gold electrodes. This device demonstrates lower intensity peaks within the bias window. While on the other hand, Au-$C_{14}H_{10}$-Au device the conduction is through HOMO for the applied voltage bias range. This device exhibits higher intensity peaks, however, the peaks are observed to be outside the window bias. The HLGs at variegated bias range for the two devices have been plotted in figure 7 and are relatively compared for both the molecular junction wires.

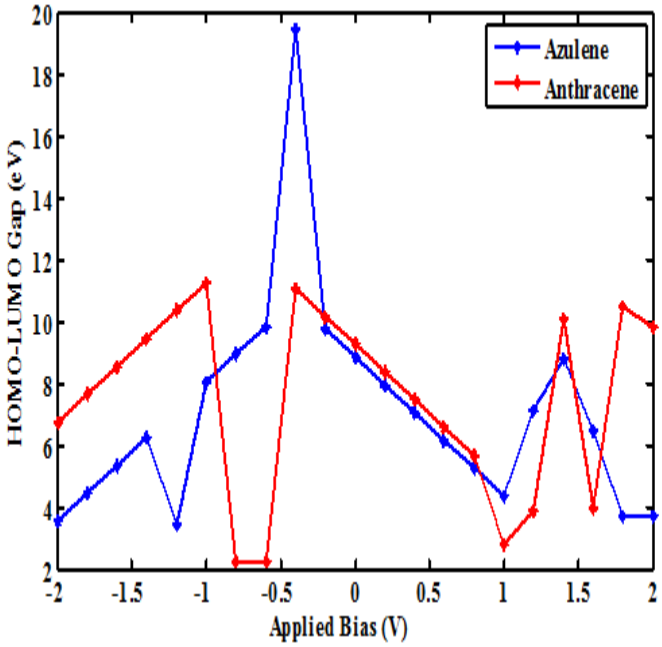

Figure 7. HOMO-LUMO gap (HLG) for Azulene and Anthracene molecular configurations under applied bias voltage range.

From the figure 7, it is obvious that for Au-Azulene-Au device, the HOMO-LUMO gap is largest at -0.4 V as compared to other device. Larger HLG leads to more stable molecular device, which is also visible from the transmission spectra. We observe that at -0.8 V and -0.6 V, the Au-$C_{14}H_{10}$-Au device shows lower HLG in comparison to Azulene based molecular configuration. Moreover, the characteristic curve exhibiting HLG for Anthracene molecular junction is quite unusual showing irregularities in its values. The molecular orbitals responsible at different bias voltages are tabulated in Table 1.

Table 1 Active molecular orbital levels at different bias voltages

Appliled Voltage in Volts	**Au-Azulene-Au**	**Au-Anthracene-Au**
-2	HOMO	HOMO
-1.8	HOMO	HOMO
-1.6	HOMO	HOMO
-1.4	HOMO	HOMO
-1.2	HOMO	HOMO
-1	HOMO	HOMO
-0.8	HOMO	LUMO
-0.6	HOMO	HOMO
-0.4	HOMO	LUMO
-0.2	LUMO	LUMO
0	LUMO	LUMO
0.2	LUMO	LUMO
0.4	LUMO	LUMO
0.6	LUMO	LUMO
0.8	LUMO	LUMO
1	LUMO	LUMO
1.2	HOMO	HOMO
1.4	LUMO	LUMO
1.6	LUMO	HOMO
1.8	LUMO	LUMO
2	HOMO	HOMO

As we can perceive from the table 1, there are three molecular orbital shifts for Au-Azulene-Au device. First shift is observed at -0.2 V, where conduction is happening through LUMO and this transmission lasts only upto +1.2 V, where conduction switches through HOMO. Last orbital shift is observed at +2 V, where transmission is through HOMO. While on the other hand, seven orbital shifts are observed for the Au-Anthracene-Au device. From -2 V to -1 V, the conduction process is through HOMO. Also at -0.6, 1.2, 1.6 and 2 V, the conduction is through HOMO. While with the rest of the applied bias voltage range, the conduction is through LUMO. The first transformation is only possible when the applied potential pushes the negative charges in molecular device. Hence its breakdown transfer of charge starts and molecular orbital changes to LUMO. The second transformation starts as soon as the increased number of participating electrons from the first breakdown get saturated which changes the active molecular orbital to HOMO. The symmetry of curve is better understood with its rectification ratio [23]. In last few years, rectification ratio for various molecular devices has been examined by many research groups and they have come up with numerous explanations [24-28]. In some devices, the

rectification ratio up to about 150 is perceived [29-31], however, frequently the current density is found very low. Single-molecule diodes have also been reported with rectification ratios (< 10) [32-35].The rectification ratio, for the two molecules is obtained for variegated bias range by dividing the current value of particular positive voltage with that of its negative voltage and is tabulated in table 2. We observe that the rectification ratio is closer to unity at extreme most voltages of 1.8/-1.8 and +2 V/-2 V for Au-$C_{10}H_8$-Au device. While for Au-$C_{14}H_{10}$-Au device, the rectification ratio is almost unity at 1.6/-1.6 V and 1.8/-1.8 V respectively.

Table 2 Rectification ratio

+V/-V	Au-Azulene-Au	Au-Anthracene-Au
0.2/-0.2	0.477	0.598
0.4/-0.4	0.177	0.714
0.6/-0.6	0.064	0.763
0.8/-0.8	0.049	0.803
1/-1	0.078	0.833
1.2/-1.2	0.325	0.873
1.4/-1.4	0.614	0.910
1.6/-1.6	0.924	1.040
1.8/-1.8	1.104	1.42
2/-2	1.426	3.76

As we move away from the intermediate voltage ratio, the rectification ratio for the two devices decreases in magnitude. Thus the two molecular configurations exhibit asymmetrical nature. Another non-equilibrium quantum parameter, current is calculated from equation 1 and plotted with respect to the applied bias voltages as shown in figure 8.

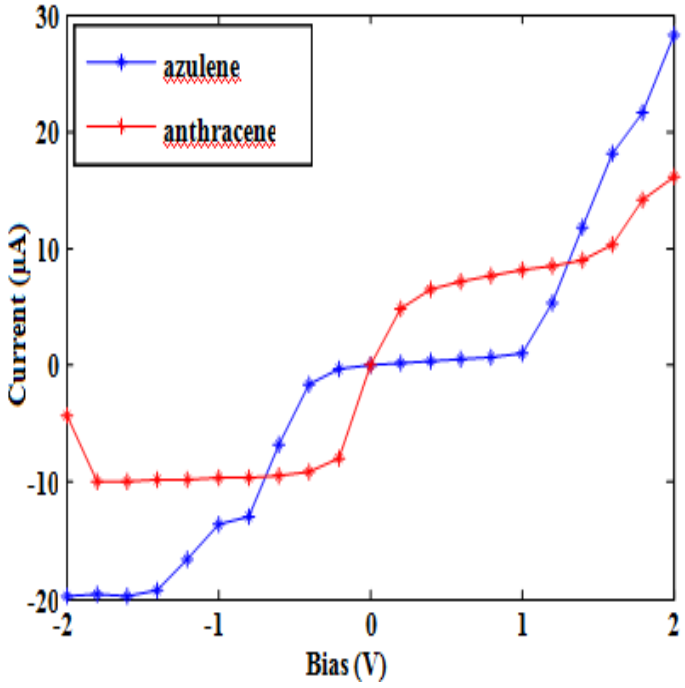

Figure 8. I-V Curve for Azulene and Anthracene molecular configurations at variegated applied biases.

The curve is divided into three segments for describing the I-V characteristics: lower bias (-0.5 V to +0.5 V), medium bias (-1.5 V to -0.5 V and +0.5 V to +1.5 V) higher bias (-2 V to -1.5 V and +1.5 V to +2 V). In lower bias segment, magnitude of the current is of linear nature for Anthracene molecular junction. This linear behaviour is due to presence of tunneling factor during conduction phenomena. Whereas, the current magnitude is almost constant within this voltage

range for Azulene molecular configuration. This is due to accumulation of charge carriers at lower bias range. In medium bias range, current characteristic for Azulene molecular device is of differential nature with stepwise increase in its magnitude. However, in Anthracene molecular configuration, conducting states are because of hybridization of this molecule with gold electrode. This conducting state results in almost constant current at negative bias range and linear type characteristics at positive bias range. At higher bias range, current tends to decrease at negative bias range and increases at positive bias range in case Anthracene molecular device, while current increases linearly for the applied bias range in case of Azulene molecular device. This practice is progressive in nature and nearly reaches to an approximate value of ±28.25 μA for 2V.The next non-equilibrium quantum parameter conductance is calculated from equation 2 and plotted with respect to the applied bias voltages as shown in figure 9. The G-V curve for the two devices is quite contradictory to its I-V graph. The conductance for Anthracene molecular device shows inelastic tunneling with Kondo peak at zero bias. The highest conductance peak at zero bias shows lifting of Coulomb blockade and leading to Kondo assisted tunneling. However, the conductance of Azulene based molecular device configuration is observed quite conflicting to its current description. The conductance of this device is lower than the other molecular device, despite being the fact that the current of this molecular device is seen higher than the anthracene based device. It is due to the fact that the HLG of Azulene based device is found to be higher at -0.4 V as compared to other device.

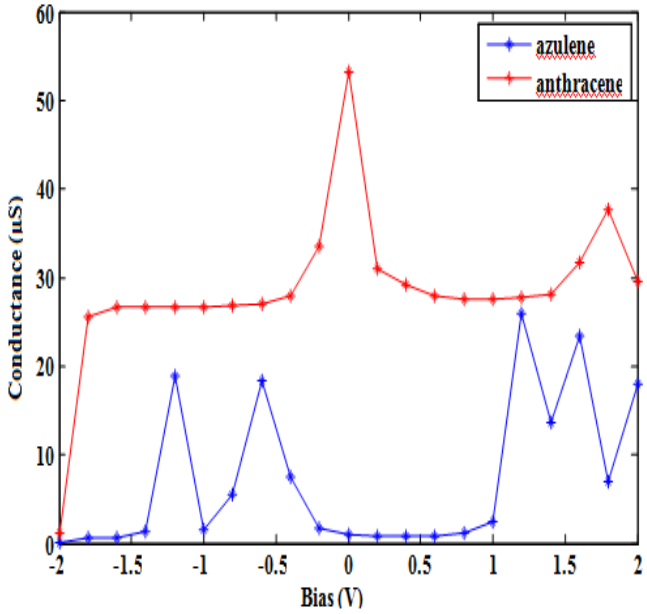

Figure 9. G-V curve for Azulene and Anthracene molecular configurations at variegated applied biases.

4. CLOSING REMARKS

In this research work, we have executed EHT and NEGF approach for both the Azulene and Anthracene molecules sandwiched between two gold electrodes to measure the quantum transport properties. We explored the various parameters like current, conductance, transmission spectra and HLG then compared those parameters for the two devices. For Azulene based device, the current magnitude is found to be higher once compared with Anthracene based device. It was due to the fact that, the transmission peaks of Azulene based device are within the bias window. Whereas the transmission peaks were found to be outside the bias window in case of Anthracene based device. Due to the lower HLG of Anthracene molecular configuration at -0.4 V, the conductance (G0) of Anthracene based device is higher as compared to Azulene based device. Moreover, At equilibrium state, transmission peaks of Anthracene based device are found within the bias window, which could predict the best projection of high

conductance. Despite the fact that conductivity of Azulene is lower as compared to Anthracene, it could be used as molecular wire in future nano-scale instruments, As this molecule exhibits higher current comparatively. Due to higher conductivity, Anthracene based molecular junction also finds its application in various molecular electronics based organic solar cells, OLEDS (organic light emitting diodes)

REFERENCES

[1] A. Aviram, and M. Ratner, Molecular Reactifiers,Chem. Phys. Lett. **29**(1974) 277–283.
[2] M. Ratner, A brief history of molecular electronics,Nature Nanotech. **18** (2013) 378–381.
[3] L. A Bumm, J. J Arnold,M. T Cygan, T. D Dunbar, T. PBurgin, L Jones, D. L Allara, J. M Tour, P. S Weiss, Are single Molecular wires conducting?,Science, **271** (1996) 1705–1707.
[4] M. A Reed, C Zhou, C. J Muller, T. P Burgin and Tour, Conductance of a Molecular Junction, J. M. Science, **278** (1997) 252–254.
[5] B Xu, and N. Tao, Measurement of Single-Molecule Resistance by Repeated Formation of Molecular Junctions, J.Science, **301** (2003) 1221–1223.
[6] N. J. TAO, Electron transport in molecular junctions,Nature Nanotechnology, **1** (2006) 173-181.
[7] Rupan Preet Kaur, Ravinder Singh Sawhney,Derick Engles, Effect of gold electrode crystallographic orientations on charge transport through aromatic molecular junctions, Molecular physics, **114** (2016) 2289-2298.
[8] Ravinder Singh Sawhney and Rupan Preet Kaur, Proliferating Conductance through Geometry Augmentation, Journal of Computational and Theoritical Nanoscience, **11**(2014) 1252-1257.
[9] Sudipta Dutta, S Lakshmi and Swapan K Pati, Comparative study of electron conduction in azulene and naphthalene, Bull Mater. Sci., **31** (2008) 353-358.
[10] Simone Piccinin, Theoretical Modeling of Electronic Transport in Molecular Devices, A dissertation presented to the faculty of princeton university in candidacy for the degree of doctor of philosophy recommended for acceptance by the department of chemistry September, 2006.
[11] Rajan Vohra, Yogita Bhat, Milanpreet Kaur, and Ravinder Singh Sawhney, Scrutiny of Electron Transport Properties of Adenine Molecule Under Dissimilar Miller Orientations J. Bionanosci. **11** (2017) 363–369.
[12] Yogita bhat , Rajan Vohra, Milanpreet kaur and Ravinder Singh Sawhney, Impact of Different Metallic Electrodes on Quantum Transport Through Deoxyribonucleic Acid, Journal of Computational and Theoretical Nanoscience, **14**, 8 (2017) 4137-4142.
[13] Yongqiang Xue, Mark A. Ratner,Theoretical Principles of Single-Molecule Electronics: A Chemical and Mesoscopic View, Quantum Chemistry, **102** (2005) 911-924.
[14] Hannu Hakkinen, The gold–sulfur interface at the nanoscale, Nature Chemistry, **l4** (2012) 443–45.
[15] G. Li and P. Miao, Theoretical Background of Electrochemical Analysis,Electrochemical Analysis of Proteins and Cells, Springer Briefs in Molecular Science, (2012) 5-18.
[16] D. Kienle,J. I. Cerda, A. W. Ghosh, Extended Hückel theory for band structure, chemistry, and transport. I. Carbon nanotubes, Journal Of Applied Physics, **100** (2006) 3714.
[17] A.Batra, P.Darancet, Q.Chen, J. S.Meisner, J. R.Widawsky, J. B.Neaton, C.Nuckolls, and L. Venkataraman,Tuning rectification in single-molecular diodes,Nano Lett., **13** (2013) 6233-6237.
[18]S. Datta, Nanoscale Device Simulation: The Green's Function Method, Superlattices and Microstructures, **l28** (2000) 253-278.
[19] S. Datta, Non-Equilibrium Green's Function (NEGF) Formalism: An elementary Introduction, Proceedings of the International Electron Devices Meeting (IEDM), IEEE Press (2002).
[20] S. Datta, Electrical resistance: an atomic view, Nanotechnology, **15** (2004) S433-S451.

[21] K. Stokbro, First-principles modeling of electron transport,J. Phys.: Condens. Matter, **20** (2008) 4216.
[22] Atomistix Tool Kit Manual Version 13.8.2 Copyright Quantum Wise 2008–2016.
[23] L.H Wang,Y. Guo, C. F. Tian, X. P. Song and B. J. Ding,Effect of the indices of crystal plane of gold electrodes on the transport properties of C_{20} fullerene, Journal of applied Physics, **107** (2010) 3702.
[24] Eldon G. Emberly and George Kirczenow, The Smallest Molecular Switch, Phys. Rev. Lett, **91** (2003) 8301.
[25] R. M. Metzger, B.Chen, U.H opfner, M. V.Lakshmikantham, D.Vuillaume, T.Kawai, X. Wu, H.Tachibana, T. V. Hughes,H.Sakurai, J. W.Baldwin, C.Hosch, M. P.Cava,L.Brehmer, G.Ashwell, J. Unimolecular electrical rectification in hexadecylquinoliniumtricyanoquinodimethanide, J. Am. Chem. Soc, **119** (1997) 455.
[26] R. M. Metzger, Unimolecular electrical rectifiers,Chem. Rev., **103** (2003) 3803-3834.
[27] J.Kushmerick, D.Holt, J.Yang, J.Naciri, M. Moore and R.Shashidhar, Metal-molecule contacts and charge transport across monomolecular layers: Measurement and theory,Phys. Rev. Lett, **89** (2002) 6802.
[28] C. M.Gu´edon, H.Valkenier, T.Markussen, K. S.Thygesen, J. C. Hummelen and S. J van der Molen, Observation of quantum interference in molecular charge transport,Nature Nanotech. **l7** (2012) 305.
[29] G. J. Ashwelland A.Mohib, Improved molecular rectification from self-assembled monolayers of a sterically hindered dye,J. Am. Chem. Soc., **127** (2005) 16238-16244.
[30] C. A.Nijhuis, W. F.Reus, J.Barber, M. D. Dickey and G. M .Whitesides, Charge transport and rectification in arrays of SAM-based tunneling junctions,Nano Lett., **10** (2010) 3611-3619.
[31] N.Nerngchamnong, L.Yuan, D. C.Qi, J.Li, D. Thompson and C. A. Nijhuis, The role of van der Waals forces in the performance of molecular diodes,Nature Nanotech., **8** (2013) 113-118.
[32] M.Elbing, R.Ochs, M.Koentopp, M.Fischer, C. Von Hanisch, F.Weigend, F. Evers, H. B. Weber and M.Mayor, A single-molecule diode,Proc. Natl. Acad. Sci. U.S.A., **102** (2005) 8815-8820.
[33] I.D´ıez-P´erez, J.Hihath, Y.Lee, L.Yu, L.Adamska, M. A. Kozhushner, I. I. Oleynik and N.J. Tao, Rectification and stability of a single-molecule diode with controlled orientation,Nat. Chem., **1** (2009) 635.
[34] E.Lortscher, B.Gotsmann, Y.Lee, L. P. Yu,C. Rettner and H. Riel,Transport properties of a single-molecule diode,ACS Nano, **l6** (2012) 4931-4939.